



*Supplement of*

## **The Canadian Atmospheric Model version 5 (CanAM5.0.3)**

**Jason Neil Steven Cole et al.**

*Correspondence to:* Jason Neil Steven Cole ([jason.cole@ec.gc.ca](mailto:jason.cole@ec.gc.ca))

The copyright of individual parts of the supplement might differ from the article licence.

## S1 Global mean statistics of cloud radiative effect for CanAM

The global mean bias, root mean square error (RMSE) and Pearson correlation coefficient is shown in Fig. S1 for the cloud radiative effect. As suggested by the zonal mean plots in Fig. 7, relative to CERES EBAF data, CanAM5 has a reduced bias and RMSE and increased correlation compared to CanAM4.

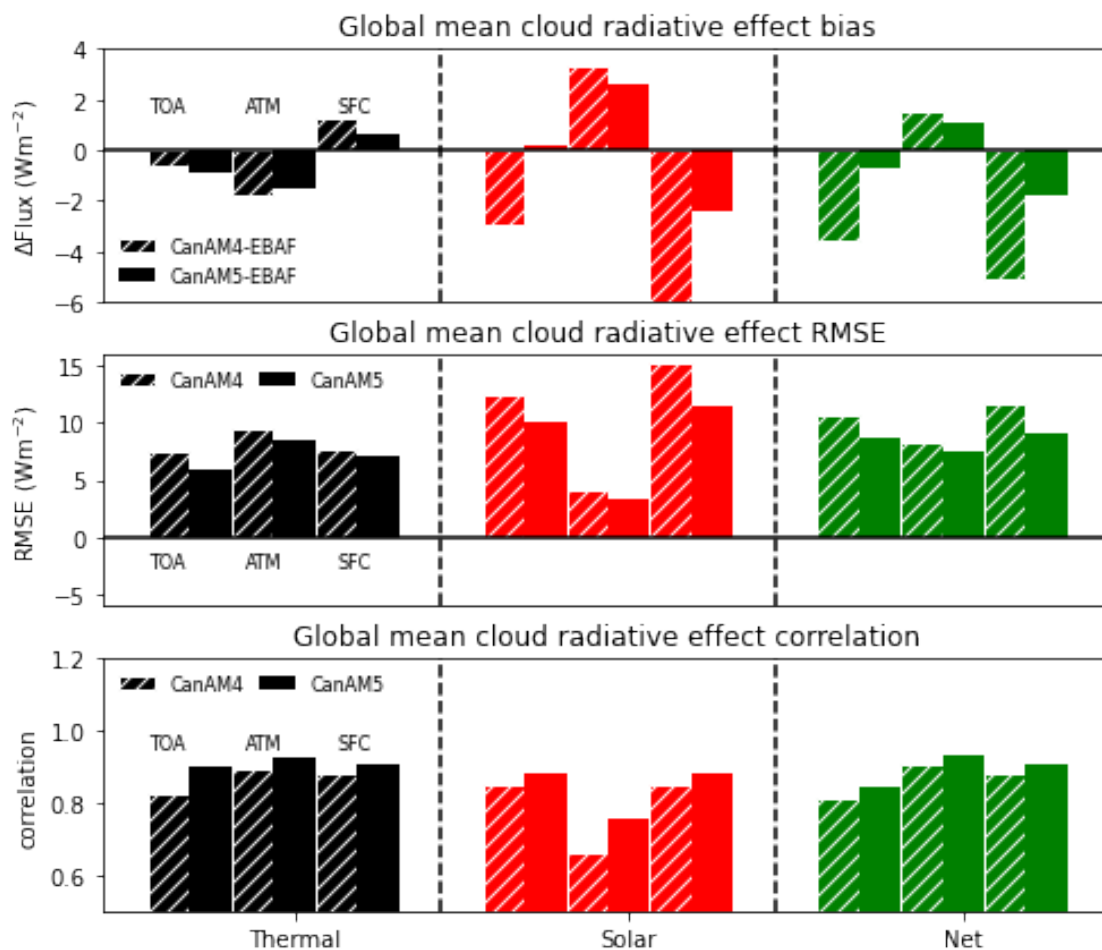


**Figure S1.** Annual global mean cloud radiative effects at the top of atmosphere, surface and atmosphere simulated by CanAM compared to CERES EBAF observations. Top row is the mean bias, middle row is the root mean square error and the bottom row is the correlation coefficient. Statistics are computed using the annual means over 2000-2005.

## 5 S2 Evaluation of CanESM5 climatology

We also reproduce here the figures from Section 6 in which we evaluate CanAM5 but instead of using CanAM4 and CanAM5 simulations with prescribed observed sea-surface temperatures (SSTs) and sea-ice we use coupled simulations in which SSTs and sea-ice evolves. In place of CanAM5 we use the first ensemble member of CanESM5 (r1i1p2f1) and in place of CanAM4 we use CanESM2 (r1i1p1) which, respectively, use CanAM5 and CanAM4 for their atmospheric model component.

- 10 Unlike the CanAM4 AMIP simulations which end in 2009, the CanESM2 historical simulations end in 2005. For some of the figures shown below, the time period to compute the means has been modified to end in 2005. This has little qualitative effect on the evaluations with observations nor the changes between CanESM2 and CanESM5.

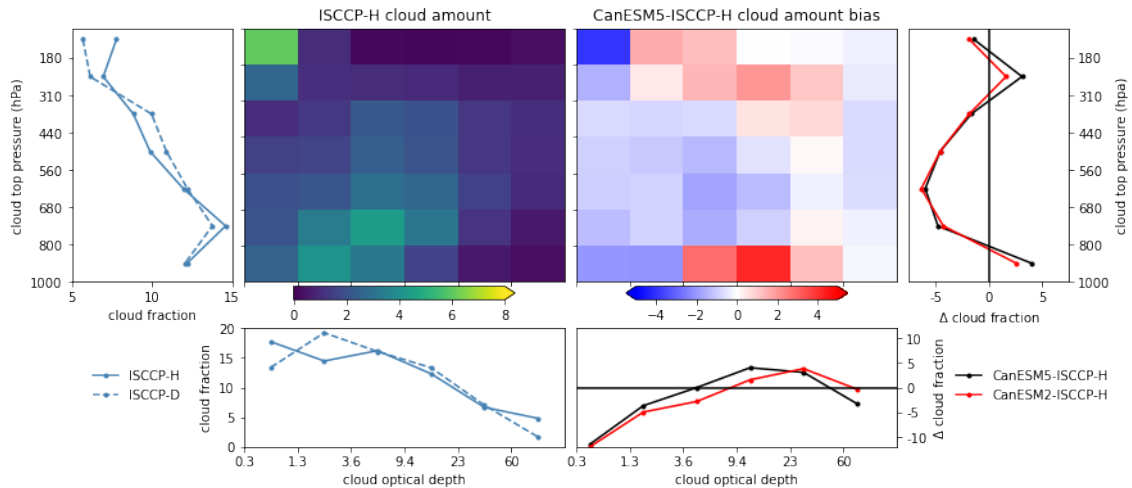


**Figure S2.** Mean histograms of the cloud fraction equatorward of  $60^\circ$  as a function of the cloud top pressure and cloud visible optical thickness from ISCCP-H and the biases in CanESM5 (mid panels in the upper row). To the side of each histogram is the mean cloud fraction, or cloud fraction bias, as a function of cloud top pressure, while below each histogram is shown the cloud fraction, or cloud fraction bias, as a function of cloud optical thickness. Means are averages for 1987-2005.

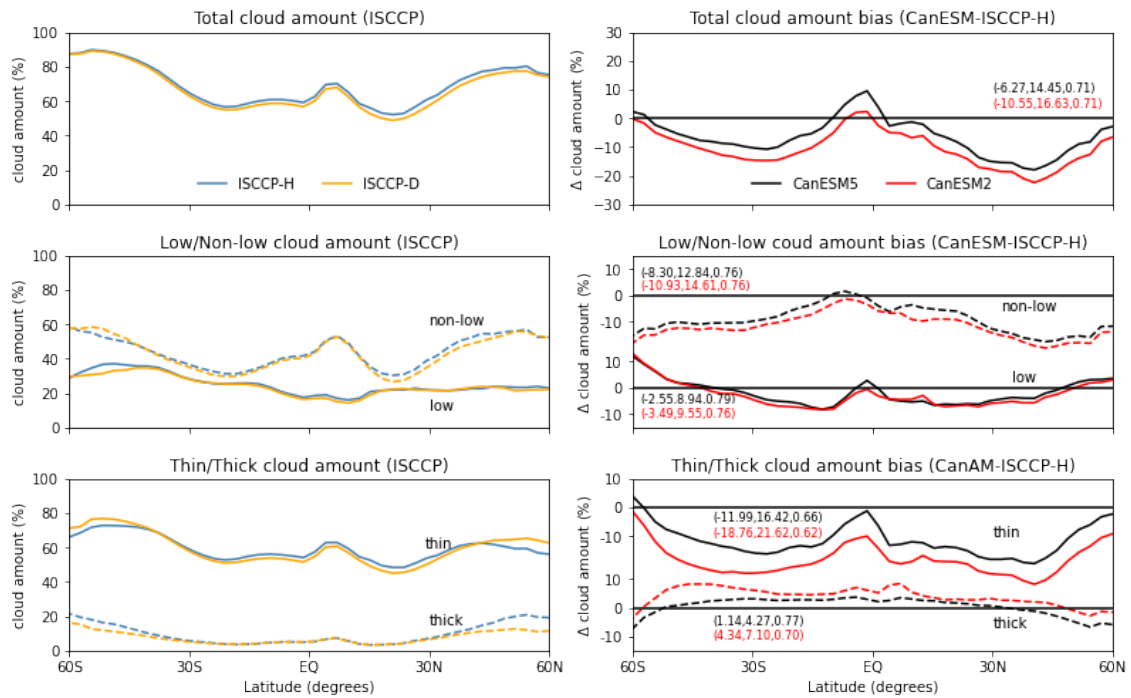


**Figure S3.** Zonal mean cloud fraction for the total cloud amount with  $\tau > 0.3$  (upper row), cloud amount for low (cloud top pressure  $> 680$  hPa) and non-low (cloud top pressure  $< 680$  hPa) in the middle row, and the cloud amount for thin (cloud visible  $\tau$  between 0.3 and 23) and thick (cloud visible  $\tau > 23$ ) in the bottom row. Observations for ISCCP-H and ISCCP-D are shown in the left column, and biases for CanESM5 and CanESM2 relative to ISCCP-H in the right column. Bracketed numbers in the right column plots are, respectively, mean bias, root mean square error and Pearson correlation coefficient, computed over the period 1987-2005 and from  $60^\circ\text{S}$  to  $60^\circ\text{N}$ , with black font for CanESM5 and red font for CanESM2.

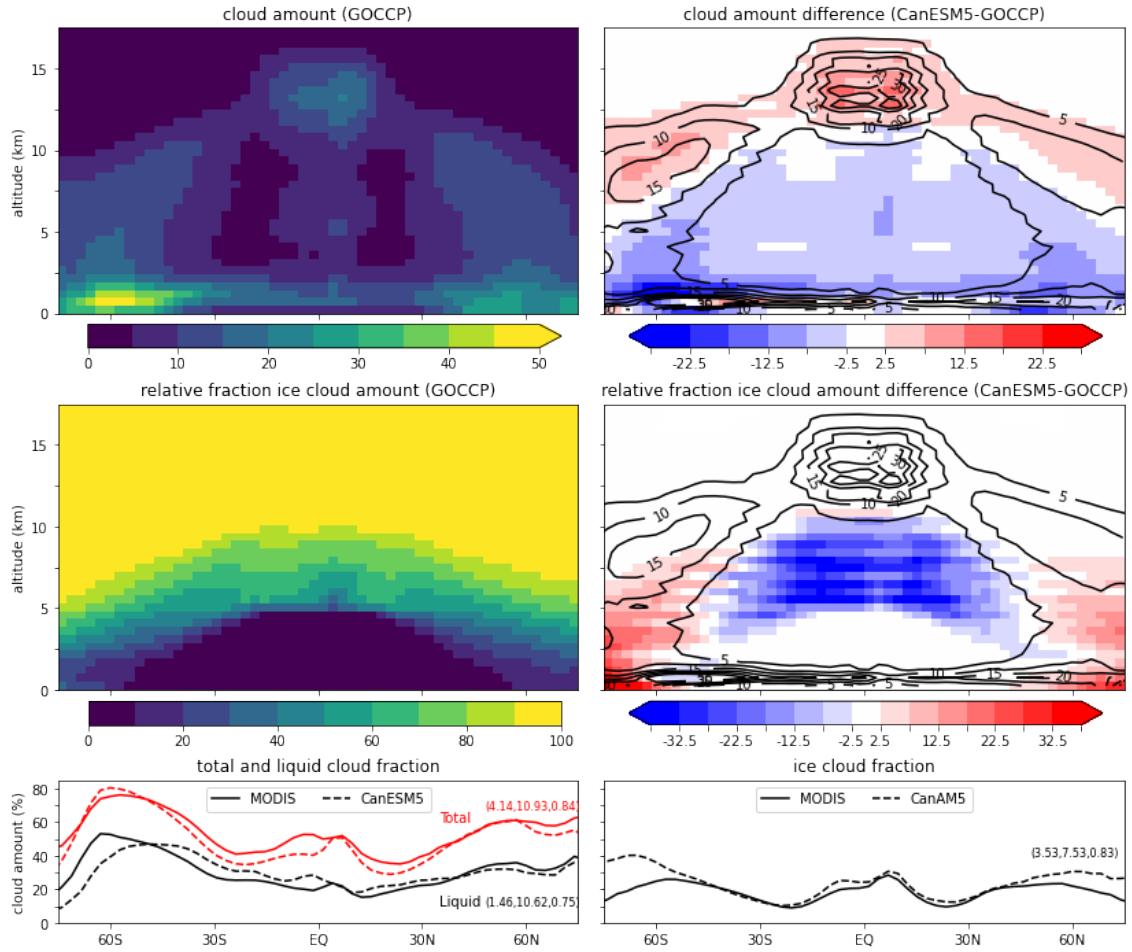


**Figure S4.** Zonal cloud fraction and cloud phase from CanESM5 compared with GOCCP and MODIS observations averaged over 2007-2009. Black contours on the upper and middle plots in the right column are the zonal mean cloud fraction from CanESM5. Bracketed numbers in the bottom row are, respectively, mean bias, root mean square error and Pearson correlation coefficient, computed using data between 75°S and 75°N.

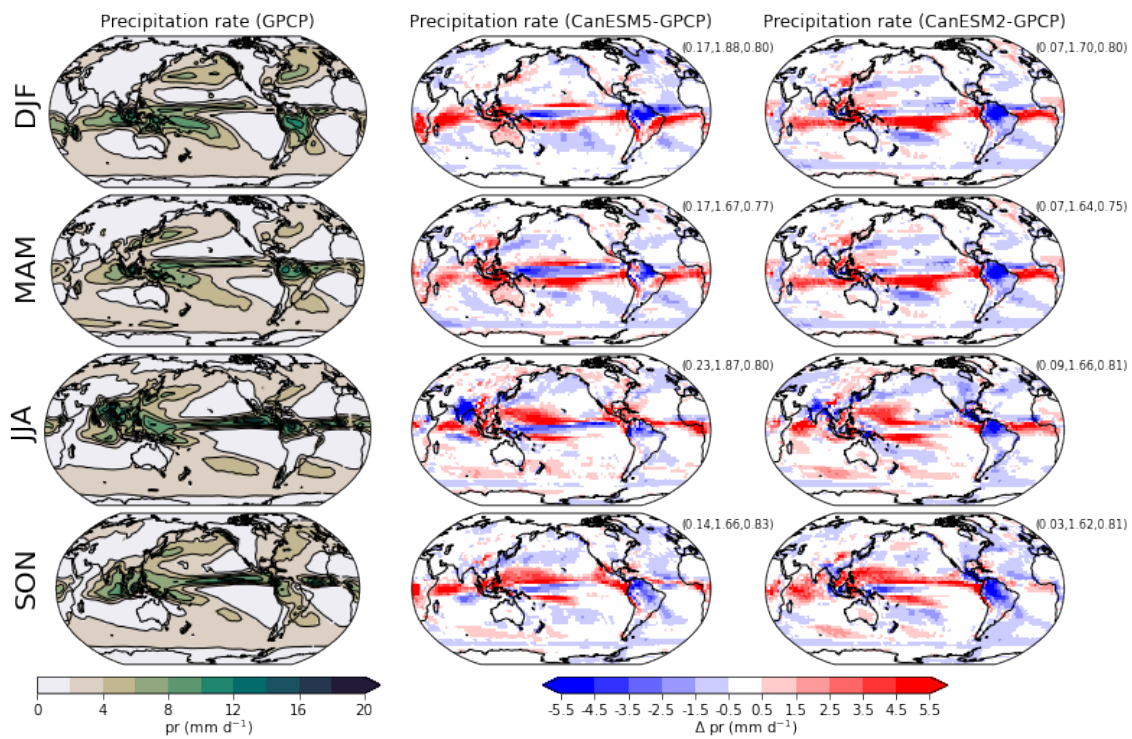


**Figure S5.** Seasonal mean precipitation rate from GPCP (left column), the bias of CanESM5 relative to GPCP (middle column) and the bias of CanESM2 relative to GPCP (right column). Bracketed numbers to the upper right of difference plots are, respectively, mean bias, root mean square error and Pearson correlation coefficient. All plots use data from years 1980-2005.

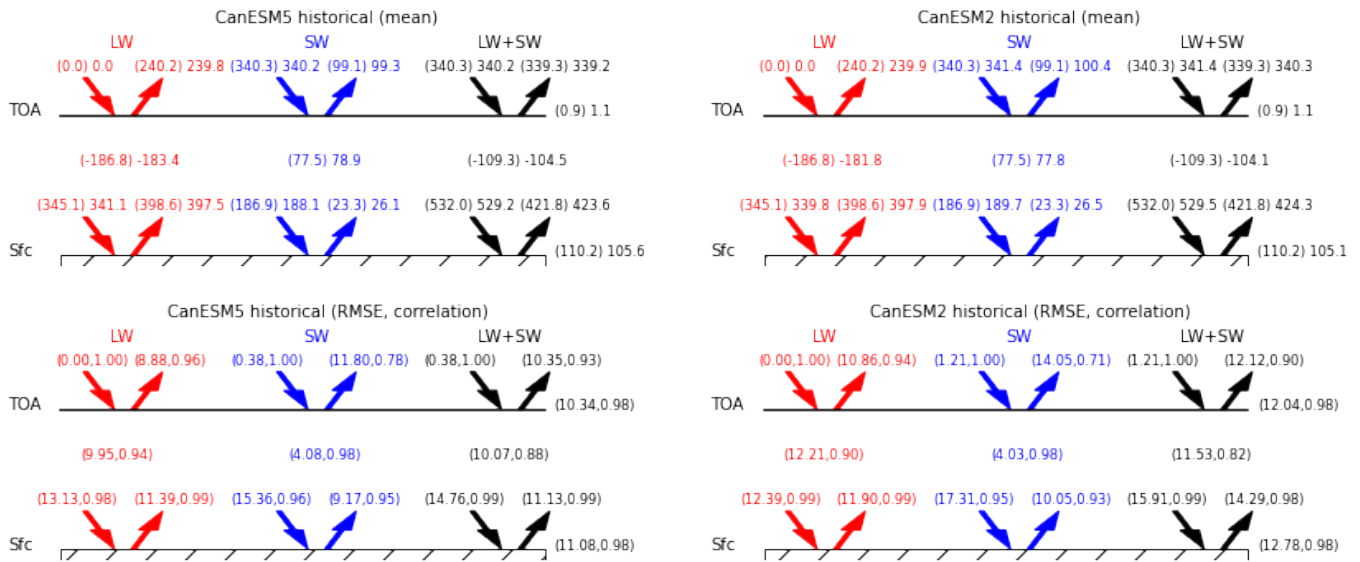


**Figure S6.** Global and time mean radiative fluxes at the top of atmosphere (TOA) and surface, as well as the net flux divergence for the atmosphere, from AMIP simulations by CanESM5 and CanESM2 compared with CERES EBAF. Statistics are computed over the period 2003-2005. For each pair of bracketed numbers in the upper row, the left value is CERES and the right value is CanESM. In the lower row, the bracketed numbers are mean bias, root mean square error and Pearson correlation coefficient of CanESM relative to CERES.

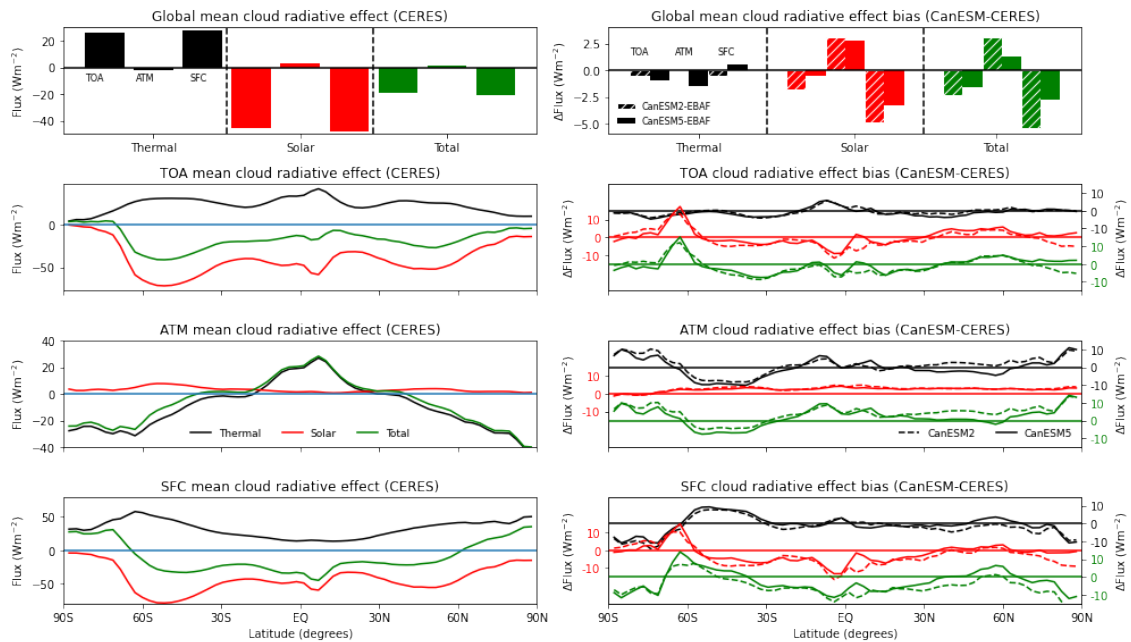


**Figure S7.** Annual global and zonal mean cloud radiative effects at the top of atmosphere, surface, and atmosphere, from CERES EBAF observation (left column) and from CanESM5 and CanESM2 historical simulations (right column). The means are averages over 2003-2005.

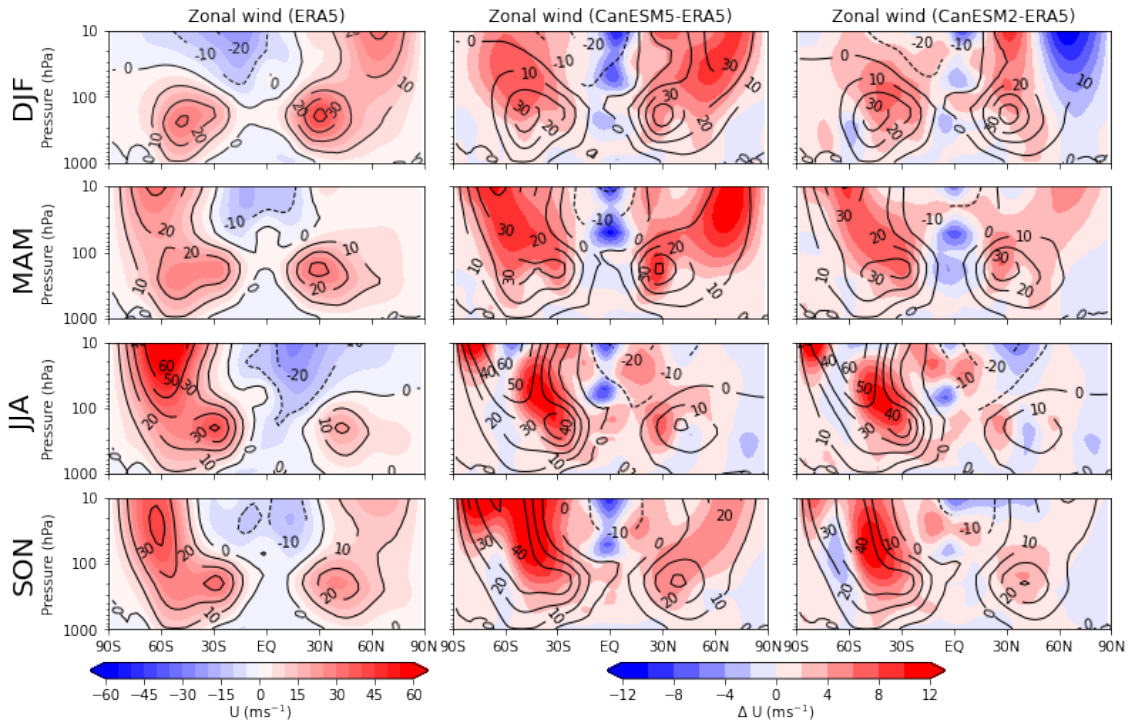


**Figure S8.** Seasonal mean latitude-pressure plots of zonal wind from ERA5 (left column), the bias of CanESM5 relative to ERA5 (middle column), and the bias of CanESM2 relative to ERA5 (right column). For all plots, contours are the mean. For the ERA5 plot, shading is the mean, in other plots the shading is the bias relative to ERA5. All plots use data from years 1980-2005.



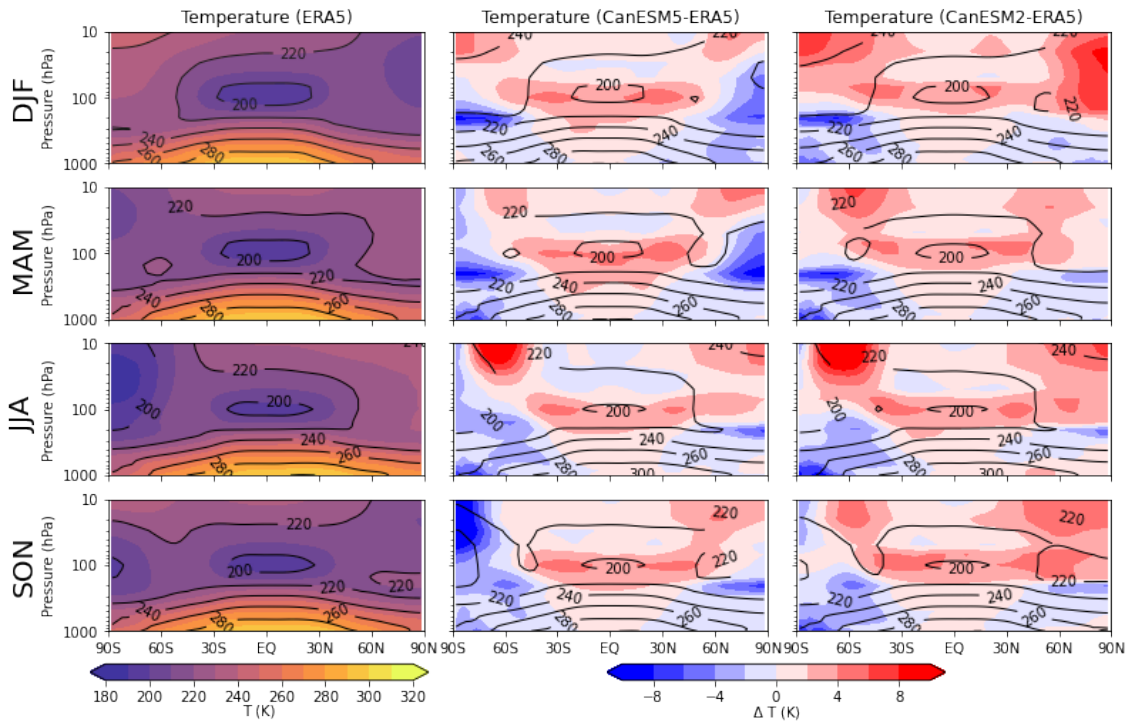


**Figure S9.** Seasonal mean latitude-pressure plots of temperature from ERA5 (left column), the bias of CanESM5 relative to ERA5 (middle column) and the bias of CanESM2 relative to ERA5 (right column). For all plots, contours are the mean. For the ERA5 plot, shading is the mean, in other plots the shading is the bias relative to ERA5. All plots use data from years 1980-2009.

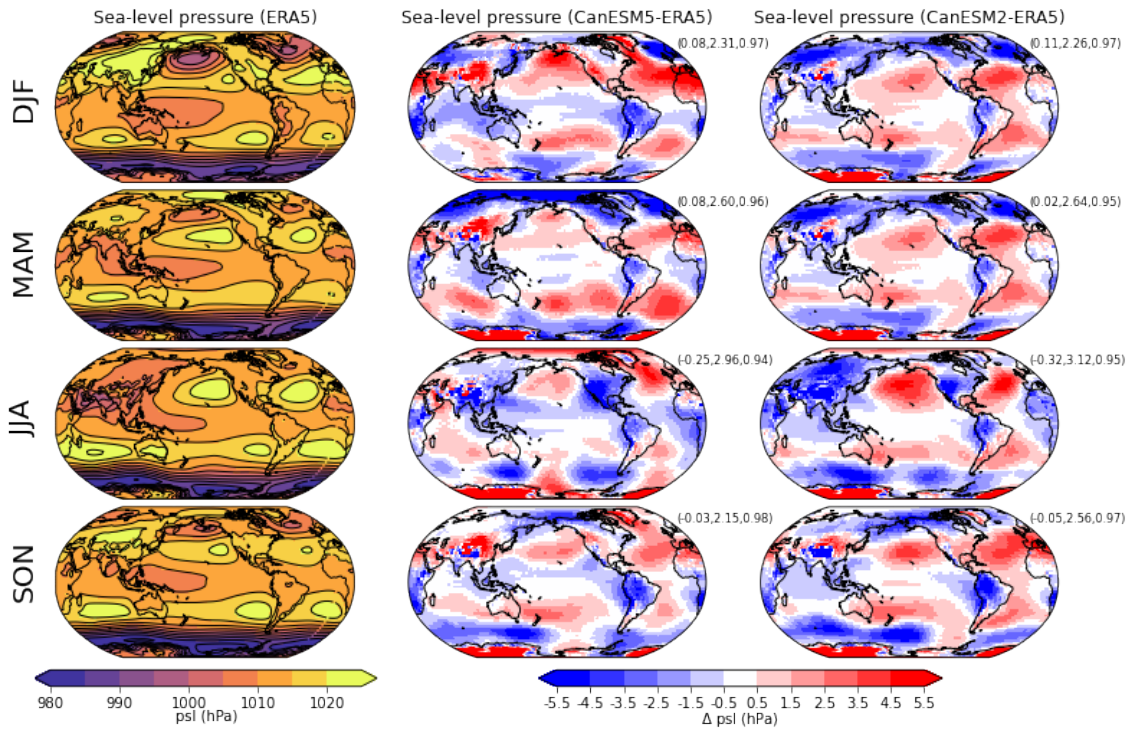


**Figure S10.** Seasonal mean sea-level pressure from ERA5 (left column), the bias of CanESM5 relative to ERA5 (middle column) and the bias of CanESM2 relative to ERA5 (right column). Bracketed numbers to the upper right of difference plots are, respectively, mean bias, root mean square error and Pearson correlation coefficient. All plots use data from years 1980-2005.

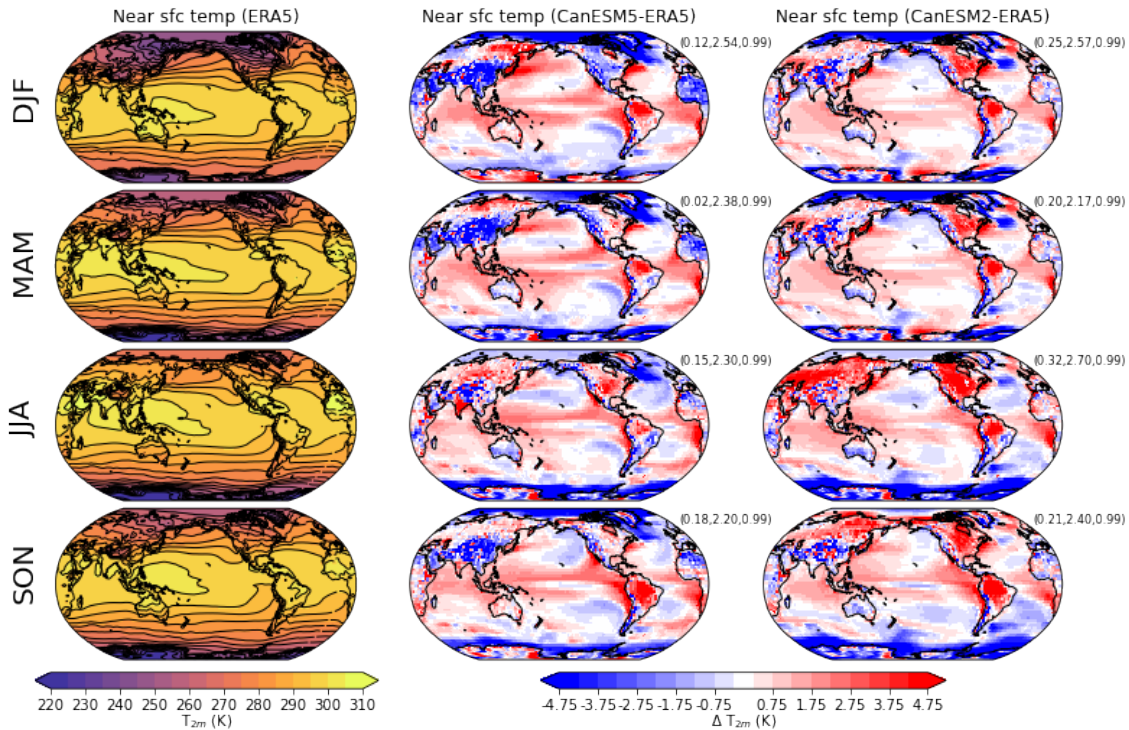


**Figure S11.** Seasonal mean near surface temperature from ERA5 (left column), the bias of CanESM5 relative to ERA5 (middle column) and the bias of CanESM2 relative to ERA5 (right column). Bracketed numbers to the upper right of difference plots are, respectively, mean bias, root mean square error and Pearson correlation coefficient. All plots use data from years 1980-2005.

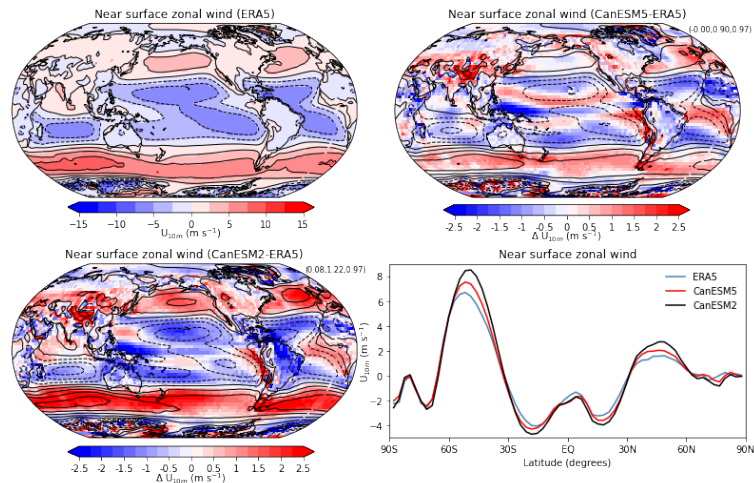


**Figure S12.** Annual mean near surface zonal wind, nominally 10 m above the surface from ERA5 (upper left) and CanESM5 and CanESM2 biases. For all plots, contours are the mean, while for the ERA5 plot shading are also the mean but in the other plots the shading is the bias relative to ERA5. Bracketed numbers to the upper right of difference plots are, respectively, mean bias, root mean square error and Pearson correlation coefficient. All plots use data from years 1980-2005.

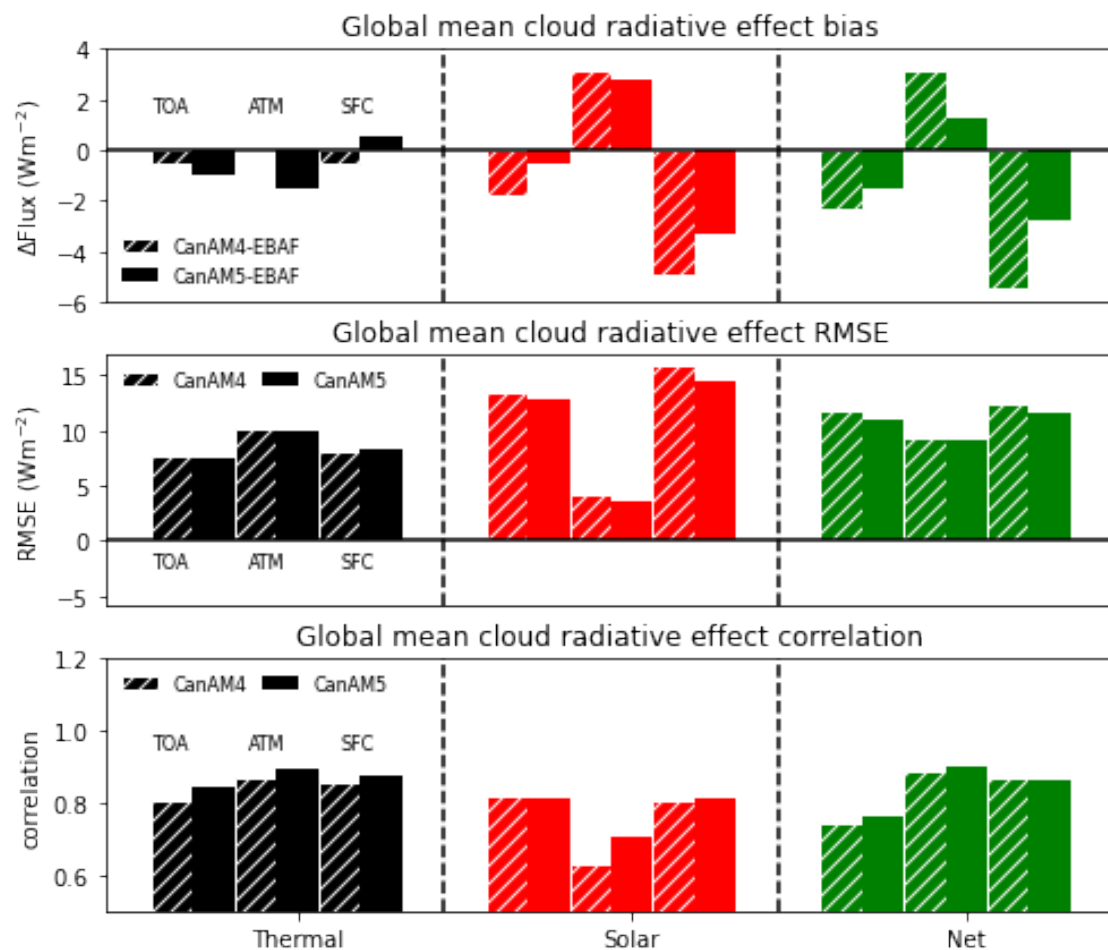


**Figure S13.** Annual global mean cloud radiative effects at the top of atmosphere, surface and atmosphere simulated by CanESM compared to CERES EBAF observations. Top row is the mean bias, middle row is the root mean square error and the bottom row is the correlation coefficient. Statistics are computed using the annual means over 2000-2005.